Reassigning Hydrogen-Bond Centering in Dense Ice

Magali Benoit,[1] Aldo H. Romero,[2] and Dominik Marx[3]

[1]*Laboratoire des Verres, Université Montpellier II, 34095 Montpellier, France*
[2]*Facultad de Fisica, Pontificia Universidad Católica de Chile, Casilla 306, Santiago 22, Chile*
[3]*Lehrstuhl für Theoretische Chemie, Ruhr–Universität Bochum, 44780 Bochum, Germany*

(Received 22 May 2002; published 10 September 2002)

Hydrogen bonds in H_2O ice change dramatically upon compression. Thereby a hydrogen-bonded molecular crystal, ice VII, is transformed to an atomic crystal, ice X. Car-Parrinello simulations reproduce the features of the x-ray diffraction spectra up to about 170 GPa but allow for analysis in real space. Starting from molecular ice VII with *static orientational* disorder, *dynamical translational* disordering occurs first via creation of ionic defects, which results in a systematic violation of the ice rules. As a second step, the transformation to an atomic solid and thus hydrogen-bond centering occurs around 110 GPa at 300 K and no novel phase is found up to at least 170 GPa.

DOI: 10.1103/PhysRevLett.89.145501 PACS numbers: 62.50.+p, 61.10.–i, 71.15.Pd, 92.40.Sn

Tuning the properties of hydrogen bonds as a function of their strength is fundamental to many processes in physics, chemistry, and life sciences. Weak or long hydrogen bonds are characterized by a pronounced double-well proton transfer potential. Upon reducing the donor-acceptor distance it degenerates via low-barrier hydrogen bonds into a single-well potential [1]. The latter leads to ''symmetric'' or ''centered'' hydrogen bonds where the protons are located midway between donor and acceptor. There is a long-standing quest to study hydrogen-bond centering in H_2O by applying pressure, thereby converting a molecular phase to an atomic phase dubbed ice X [2]. But unexpectedly, even the ''simple'' low-pressure molecular ices VII and VIII are found to be structurally much more complex [3–6] than previously accepted models [7]. At very high pressures, where centering in ice occurs, the traditional experimental probe has been vibrational spectroscopy [8–17]. Only recently it has become possible to directly probe the positions of the hydrogens by x-ray diffraction up to the Megabar regime. Starting from ice VII, this pioneering experiment [6] allowed one to follow — in reciprocal space — the pressure-induced changes of hydrogen bonds up to 170 GPa at 300 K.

Concerning centering and the formation of ''evasive ice X'' [18], however, there is a controversy in the recent literature due to the intricate pretransitional behavior [6,15–18], in particular, with respect to the centering pressure and the suggestion of a novel high-pressure phase [6]. Here, Car-Parrinello simulations [19,20] are found to reproduce the features of the experimental x-ray diffraction spectra. At room temperature orientationally disordered ice VII undergoes an additional translational disordering, which is induced by proton hopping along hydrogen bonds via transient ionic defects. Furthermore, this is a transition from frozen-in static disorder to dynamical disorder so that it manifests itself in the decay of an Edwards-Anderson–like order parameter that was introduced for spin glasses [21,22]. This scenario is similar to, but different from, low temperatures where *ordered* ice VIII is stable and proton tunneling drives disordering [23]. In addition, it is inferred that the transformation to an atomic solid and thus true hydrogen-bond centering occurs close to 110–120 GPa at 300 K and, most importantly, no novel phase occurs up to at least 170 GPa.

In a seminal synchrotron x-ray diffraction study of ice it was possible to follow the 111 and 222 reflections up to 170 GPa [6]. The 111 Bragg peak is mainly due to the hydrogens, whereas the 222 signal is dominated by the oxygen sublattice which is known to remain body centered cubic (bcc) up to very high compression [24,25]. Thus, the intensity ratio $R = I_{111}/I_{222}$ is expected to monitor changes of the hydrogen positions relative to a steadily contracting bcc reference system. The analysis [6] of the diffraction data taken at ambient temperature uncovered three regimes: two steeply rising parts at low and high pressures separated by a rather flat intermediate region; see Fig. 3 in Ref. [6].

In an effort to assign these different regimes to underlying microscopic real-space structures and transition scenarios a series of *ab initio* Car-Parrinello simulations [19,20] of ice at 300 K was launched; note that H/D isotope quantum effects are small at room temperature [8,13]. The *ab initio* Car-Parrinello molecular dynamics [19,20,26] simulation data were obtained with 16 H_2O molecules placed in a fixed-volume periodic cubic box. Kohn-Sham density functional theory was used in the framework of a gradient-corrected [27] local-density approximation. The wave function was expanded in plane waves at the Γ point using a cutoff of 70 Ry in conjunction with Troullier-Martins pseudopotentials. The temperature was fixed at 300 K in the canonical ensemble and the pressure was obtained using the most recent experimental equation of state [6]. The trajectories consist of at least 40 000 configurations, but they comprise up to

72 000 (corresponding to about 7 ps) in the crucial region between about 50 to 110 GPa; every 20th configuration was used for the analysis.

Based on the trajectories of the nuclei the energy-dispersive x-ray diffraction spectra [28,29] $I(E)$ and thus the intensity ratio $R = I_{111}/I_{222}$ was computed from about 5 to 190 GPa; see Fig. 1(a). A most economical alternative would consist in computing R using static structural models for the ice phases. Following this route it was found that the behavior of R is extremely sensitive to the atomic displacement parameters used. They account for positional fluctuations with respect to the equilibrium lattice positions in the Debye-Waller approximation, and possibly for multisite disorder. Using *ab initio* simulations, these effects are not put in by hand *a posteriori;* rather they are generated dynamically in the canonical ensemble at 300 K. Interestingly, it is found that the quadratic fluctuations σ_H^2 and σ_O^2 of both the hydrogen and oxygen atoms around their respective average positions (which are closely related to the displacement

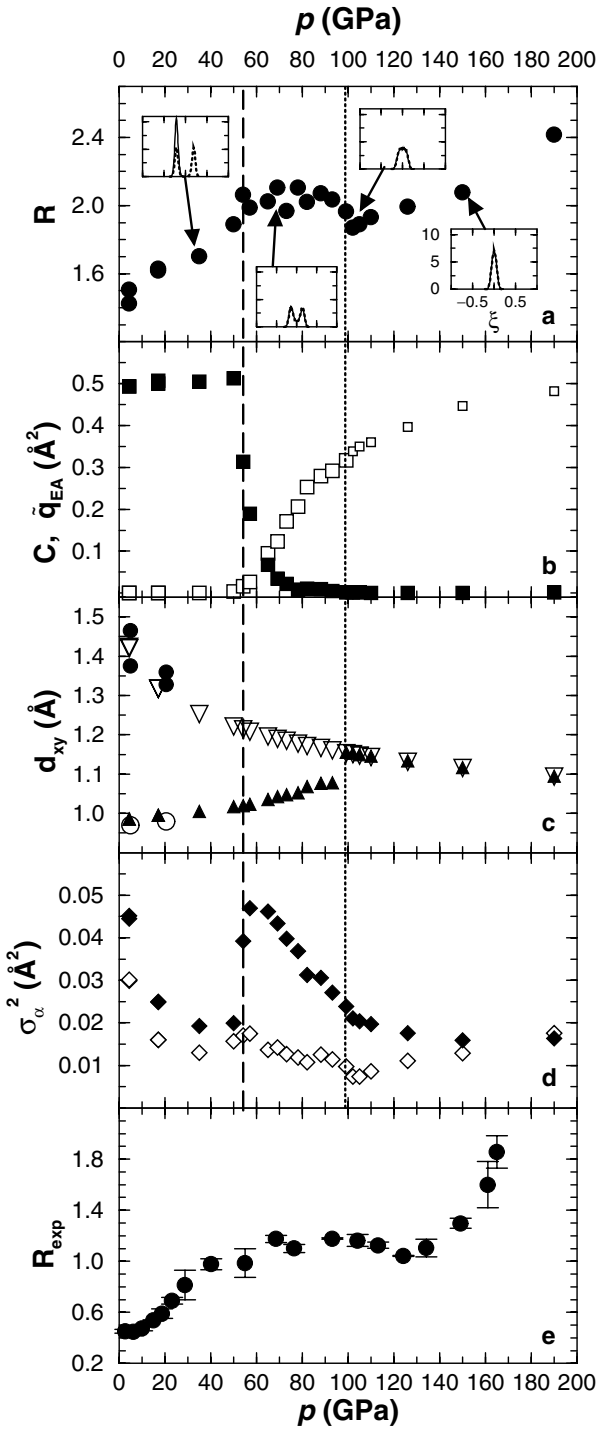

FIG. 1. Properties of ice at 300 K as a function of pressure. (a) Intensity ratio $R = I_{111}/I_{222}$ (filled circles) and representative proton densities $P(\xi)$ (insets) averaged over all O_aHO_b atom triples where $\xi = (d_{O_aH} - d_{O_bH})/d_{O_aO_b}$ and $\int d\xi P(\xi) = 1$ for all insets. For each O_aHO_b triple the corresponding sign of ξ is defined based on both the *fictitious* antiferroelectric sublattices that would correspond to ice VIII at low temperatures (dotted lines) and on the actual random static orientational disorder configuration of paraelectric ice VII that was used to initialize the particular simulation (solid lines). (b) Scaled Edwards-Anderson order parameter $\tilde{q}_{EA} = q_{EA}/10$ (filled squares) and relative number of defects $C = \langle n_{broken}\rangle/n_{sites}$ (open squares) obtained as the number of broken water molecules (based on a geometric criterion) normalized by the number of available lattice sites; note that C ultimately becomes ill-defined in centered ice (small open squares). (c) Oxygen-hydrogen d_{OH} (filled up-triangles) and half the oxygen-oxygen $d_{OO}/2$ (open down-triangles) distances as obtained from the first moment of the corresponding distribution functions. Experimental values [4] of d_{OH} (open circles) and $d_{OO}/2$ (filled circles) within the $\langle 111\rangle$ site-disordered model of D_2O at 288 K are also shown. (d) Mean-square displacements $\sigma_\alpha^2 = (1/N_\alpha)\sum_{I_\alpha=1}^{N_\alpha}\langle(\mathbf{R}_{I_\alpha} - \langle\mathbf{R}_{I_\alpha}\rangle)^2\rangle$ for $\alpha = H$ (filled diamonds) and $\alpha = O$ (open diamonds) atoms with respect to their respective average positions $\langle\mathbf{R}_{I_\alpha}\rangle$. (e) Reanalyzed experimental intensity ratio [6] obtained as the average $R = (I_{111}/I_{222} + I_{11\bar{1}}/I_{22\bar{2}})/2$ (circles) of the indicated hkl and $hk\bar{l}$ reflections for fixed $2\theta = 11.67°$; I_{111}/I_{222} and $I_{11\bar{1}}/I_{22\bar{2}}$ are shown by the error bar symbol. In (a)–(d) the vertical dashed lines are at $p \approx 55$ GPa, where C [panel (b)] increases strongly and the vertical dotted lines are at $p \approx 100$ GPa, where d_{OH} and $d_{OO}/2$ [panel (c)] become identical. At about 5 and 20 GPa two statistically independent data points are depicted in (a)–(d) which correspond to two static disorder configurations of molecular ice VII.

parameters) display a pronounced nonmonotonous behavior that parallels the underlying structural transformations; see Fig. 1(d). In particular, the jump of σ_H^2 around 55 GPa signals the onset of dynamical site disordering of the hydrogens at that pressure in addition to static orientational disorder below. A similarly rich behavior was already uncovered at lower pressures [4]. Thus, calculations of the intensity ratio R using *rigid* lattices in conjunction with *fixed* atomic displacement parameters are not expected to describe the subtle features that unfold during hydrogen-bond compression.

In addition to reciprocal space information in terms of Bragg peaks *ab initio* simulations provide detailed insights into the corresponding real-space properties. In particular, the relative number of ionic defects C and the average length of the OH and OO bonds, d_{OH} and d_{OO}, are displayed in Figs. 1(b) and 1(c), respectively. The concentration of defects C is estimated by determining the relative number of "broken" water molecules; i.e., those that do not have two hydrogens attached to them. Detailed analysis of the corresponding distribution function shows that these broken water molecules are mainly of the type of formal H_3O^+ and OH^- charge defects. In the low-pressure regime the number of broken water molecules is negligible, whereas a sudden and significant increase is detected around 55 GPa; see Fig. 1(b). This implies that the ice rules [7] are satisfied below this transformation, while they are *systematically* violated above it. Thus, an "ionization transition" takes places at this pressure [where $d_{OO} \approx 2.4$ Å as inferred from Fig. 1(c)] similar to the one obtained earlier in the low-temperature limit [23,31]; see, however, the discussion below.

It is interesting to analyze in more detail the nature of the ionization transition. For this purpose we introduce an Edwards-Anderson–like order parameter [21,22] $q_{EA} = [\sum_I \langle \mathbf{d}_I \rangle^2 / N]_{av}$, where the spin variable $\mathbf{S}_I$ is replaced by the geometric dipole moment vector [23] $\mathbf{d}_I$ computed at each lattice site. This order parameter allows one to detect *dynamical* disordering setting in on top of frozen-in static *disorder* where q_{EA} is large. A well-known case is spin glasses [22] undergoing a glass transition upon heating; note that *both* states do not show any magnetic order; i.e., the magnetic order parameter $D' = [\langle | \sum_I \mathbf{d}_I | \rangle / N]_{av} = 0$ vanishes. In ice, q_{EA} is found to be large up to about 55 GPa, where a sudden decay sets in at the same pressure where C rises steeply [see Fig. 1(b)]; note that $\tilde{q}_{EA} = q_{EA}/10$ was *scaled* in order to display it on the same scale as C. Since the sample at 300 K is paraelectric both below and above this transition (i.e., the antiferroelectric order parameter [23] D is small, not shown) the decay of q_{EA} implies that the disorder is static at low pressures, whereas the ionized phase is characterized by *dynamical* disorder.

The average OH bond length d_{OH} increases smoothly up to about 100 GPa; see Fig. 1(c). At this pressure, the point is reached where d_{OH} amounts to half the OO distance $d_{OO}/2$ with $d_{OO} \approx 2.3$ Å. This is exactly what defines physically centering of hydrogen bonds in the classic sense of Huggins [32] and Holzapfel [33]. For ice this leads to the cuprite Cu_2O structure [2] as sketched, e.g., in Fig. 1 of Ref. [10] and also found in previous low-temperature simulations at highest compressions [23]. This implies that between about 55 and 100 GPa—although many water molecules are broken—the protons nevertheless prefer to reside closer to one of their two neighboring oxygen atoms. Thus, based on these simulation data the hydrogen bonds can be considered centered only for pressures exceeding about 100 GPa.

This three-stage scenario "molecular → ionized → centered" can be clearly distinguished visually using the averaged proton distribution function $P(\xi)$ where ξ defines the relative position of a given proton between its two neighboring oxygens scaled such that the latter are located at $\xi = \pm 1$ and $\xi = 0$ implies the bond-centered situation. Following the evolution of $P(\xi)$ allows one to analyze rigorously centering in the spirit of Schweizer and Stillinger [31]; see the insets in Fig. 1(a). Only above 100 GPa, the proton density is found to be unimodal with one peak at $\xi = 0$ thus yielding the cuprite structure [2] as the isomorphic structure in the static limit, whereas $P(\xi)$ displays two peaks at $|\xi| \neq 0$ for lower pressures. Below about 55 GPa these peaks are clearly separated, indicating that the protons remain attached to a given oxygen. This is in strong contrast to the behavior in the ionized regime between 55 and 100 GPa. Here, the protons exchange their position constantly by traveling forth and back along their hydrogen bonds resulting in *dynamical translational* proton disorder. As already discussed [18] the emerging structure is *not isostructural* to the static cuprite structure [2]. The crucial difference is that in both the ionized and centered phases the *average* proton position is the bond center, but only in the centered phase the bond center is also the *most probable* position; see the insets in Fig. 1(a). Since the disordering mechanism is mediated by mainly H_3O^+ and OH^- ionic defects, see Fig. 1(b), this imposes some local correlations that prevent unconstrained disorder. This view is consistent with the speculation [4] that the ionized regime could represent a mixed intermediate state in which proton disorder progressively develops in bonds of different lengths.

At first glance this room temperature scenario seems to be similar to what was inferred in the low-temperature limit [23,31]. However, the initial phase at 300 K, paraelectric ice VII, is orientationally disordered when *additional* translational disordering sets in, whereas below 100 K it is antiferroelectrically ordered ice VIII that undergoes directly translational disordering. Thus, it is a transition from static disorder to dynamic disorder at 300 K, whereas it is an order-disorder transition at low temperatures. Interestingly, this suggests that in between 100 and 280 K the transition line found in experiments [8,14] (see Figs. 2 and 1 therein, respectively) is an

orientational disordering transition of ice VIII to molecular ice VII that is mediated by Bjerrum defects [7]. In addition, the ionization transition is driven by tunneling at low temperatures [23], whereas thermally activated hopping is the main channel at room temperature as found out by explorative path integral simulations at 300 K.

The behavior of all microscopic quantities in Figs. 1(b)–1(d) parallels closely the evolution of the intensity ratio R in Fig. 1(a). There is an upwards-curved increase up to about 55 GPa where $R \approx 2$. At this point (dashed line), R starts to bend downwards and reaches again the same value of $R \approx 2$ at approximately 100 GPa thus forming a "hump" in this regime just before a local minimum occurs. There, a rather steep upwards-curved increase sets in upon further compression. Thus, the low-pressure wing of the hump separates a molecular regime of ice VII from an ionized regime where a large fraction of the covalent OH bonds is broken. This intermediate ionized regime is predicted to display a pronounced dielectric response in experiment. Finally, bond centering occurs only at the high-pressure wing of the hump at about 100 GPa just before R vs p actually displays its shallow minimum.

Having understood the simulation results the reanalyzed experimental data [6] can be rationalized in a new light; see Fig. 1(e). The simulations of "virtual ice" clearly capture *qualitatively* the behavior of real ice, in particular, the initial rise, the hump, the shallow minimum, and finally the steep increase of R; *quantitative* differences exist due to deficiencies of density functional theory, but, in particular, finite-size effects induced by the rather small supercell are expected to be significant in disordered systems where diffuse scattering contributes to $S(\mathbf{Q})$ and thus to R. Based on the experimental x-ray data and the microscopic theoretical understanding, it is concluded that centered ice becomes stable only at about 110–120 GPa (the experimental error [6] is of the order of ± 6 GPa at 170 GPa taking into account the uncertainty of the ruby scale). This implies that the steep increase of R after about 120 GPa is a feature of ice X and no evidence for a new phase. This reassignment—made possible by combining experiment and simulation—reconciles conflicting interpretations of diffraction and spectroscopic experiments [6,15–17] and thus closes the chapter as to where "evasive ice X" [18] becomes the stable polymorph of water at room temperature.

We are deeply indebted to Paul Loubeyre for reanalyzing the diffraction raw data, for making them available to us, and for very helpful discussions. We gratefully acknowledge the help of Roger Rousseau and John Loveday in clarifying important technical issues. A. H. R. acknowledges the support of Fondecyt (Chile) under Grant No. 1010988. The simulations were carried out on the IBM SP at CINES (Montpellier) and at RUB (Bochum).

[1] G. A. Jeffrey, *An Introduction to Hydrogen Bonding* (Oxford University Press, Oxford, 1997).
[2] K. R. Hirsch and W. B. Holzapfel, Phys. Lett. **101A**, 142 (1984).
[3] J. M. Besson *et al.*, Phys. Rev. Lett. **78**, 3141 (1997).
[4] R. J. Nelmes *et al.*, Phys. Rev. Lett. **81**, 2719 (1998).
[5] S. Klotz *et al.*, Nature (London) **398**, 681 (1999).
[6] P. Loubeyre *et al.*, Nature (London) **397**, 503 (1999).
[7] V. F. Petrenko and R.W. Whitworth, *Physics of Ice* (Oxford University Press, Oxford, 1999).
[8] Ph. Pruzan, J. Mol. Struct. **322**, 279 (1994).
[9] K. Aoki, H. Yamawaki, and M. Sakashita, Science **268**, 1322 (1995).
[10] A. F. Goncharov *et al.*, Science **273**, 218 (1996).
[11] K. Aoki *et al.*, Phys. Rev. B **54**, 15 673 (1996).
[12] K. Aoki, H. Yamawaki, and M. Sakashita, Phys. Rev. Lett. **76**, 784 (1996).
[13] V.V. Struzhkin *et al.*, Phys. Rev. Lett. **78**, 4446 (1997).
[14] Ph. Pruzan *et al.*, J. Phys. Chem. B **101**, 6230 (1997).
[15] A. F. Goncharov *et al.*, Phys. Rev. Lett. **83**, 1998 (1999).
[16] M. Song *et al.*, Phys. Rev. B **60**, 12 644 (1999).
[17] E. Katoh *et al.*, Phys. Rev. B **62**, 2976 (2000).
[18] W. B. Holzapfel, Physica (Amsterdam) **265B**, 113 (1999).
[19] R. Car and M. Parrinello, Phys. Rev. Lett. **55**, 2471 (1985).
[20] D. Marx and J. Hutter, in *Modern Methods and Algorithms of Quantum Chemistry*, edited by J. Grotendorst (NIC, FZ Jülich, 2000), p. 301; see www.theochem.ruhr-uni-bochum.de/go/cprev.html.
[21] S. F. Edwards and P.W. Anderson, J. Phys. F **5**, 965 (1975).
[22] K. Binder and A. P. Young, Rev. Mod. Phys. **58**, 801 (1986).
[23] M. Benoit, D. Marx, and M. Parrinello, Nature (London) **392**, 258 (1998).
[24] R. J. Hemley *et al.*, Nature (London) **330**, 737 (1987).
[25] E. Wolanin *et al.*, Phys. Rev. B **56**, 5781 (1997).
[26] J. Hutter *et al.*, computer code CPMD, MPI FKF and IBM Zurich, 1995–1999.
[27] A. D. Becke, Phys. Rev. A **38**, 3098 (1988).
[28] B. Buras and L. Gerward, Acta Crystallogr. Sect. A **31**, 372 (1975).
[29] The ratio $R = I_{111}/I_{222}$ is obtained from $I_{hkl} = I_0\, \lambda_{hkl}^4\, S(\mathbf{Q}_{hkl})$ [28]; I_0 collects constant prefactors, $S(\mathbf{Q}) = (1/N)\langle|\sum_{I=1}^{N} f_I(\mathbf{Q}) \exp[-i\mathbf{Q}\mathbf{R}_I]|^2\rangle$ is computed for fixed experimental $2\theta = 11.67°$ as a function of $E = hc|\mathbf{Q}|/4\pi \sin\theta = hc/2\lambda \sin\theta$ using tabulated [30] atomic form factors f_I.
[30] *International Tables for X-Ray Crystallography*, edited by J. A. Ibers and W. C. Hamilton (Kynoch Press, Birmingham, 1974), Vol. IV.
[31] K. S. Schweizer and F. H. Stillinger, J. Chem. Phys. **80**, 1230 (1984); note that a hydrogen bond is considered to be centered if the single bond proton density is peaked at the bond midpoint.
[32] M. L. Huggins, J. Phys. Chem. **40**, 723 (1936).
[33] W. B. Holzapfel, J. Chem. Phys. **56**, 712 (1972); note that a hydrogen bond is considered to be centered if the equilibrium position of the proton is identical to the center of the bond.